Observation of coherent acoustic and optical phonons in bismuth nanowires by a femtosecond pump-probe technique

Alexandre A. Kolomenskii,[a] Sergey N. Jerebtsov, Haidong Liu, Hong Zhang, Zuxin Ye, Zhiping Luo,[b] Wenhao Wu, and Hans A. Schuessler
Department of Physics, Texas A&M University, College Station, Texas 77843-4242, USA

(Received 20 July 2008; accepted 30 September 2008; published online 19 November 2008)

Coherent acoustic and optical phonon oscillations in Bi nanowire samples were studied with a femtosecond pump-probe technique. Laser pulses of 50 fs excited *simultaneously* acoustic oscillations at a frequency of about 9.5 GHz and optical phonons in the terahertz range. The transmission signal of nanowires on a glass substrate and the signal of light scattered from freestanding nanowires were measured. The acoustic velocity in nanowires was found to be close to that of bulk polycrystalline material. The changes in the optical phonon frequency at different laser fluences were simulated taking into account excitation inhomogeneity, lattice anharmonicity, diffusion, and recombination of the carriers and gave good agreement with experimental results.
© *2008 American Institute of Physics*. [DOI: 10.1063/1.3021101]

I. INTRODUCTION

In the past, probing of scattered light proved to be a powerful tool for studies of condensed matter,[1] in particular Raman spectra of optical phonons in Bi were measured.[2] More recently, excitation of acoustic[3] and optical phonon[4–6] modes in films of different materials, including Bi,[7,8] with short laser pulses was performed. Such pulses excite all active vibrations with frequencies contained in the pulse envelope.[9] The laser light produces electronic excitations, which are coupled to the lattice vibrations via deformation potential[3] and stimulated Raman scattering.[9] After action of a short laser pulse the equilibrium positions of the nuclei are displaced, and they start oscillating around these new equilibrium positions. Thus the lattice distortions give rise to coherent acoustic and optical phonons. The excitation of the lattice oscillations of optical phonons was explained via the displacive mechanism,[10] which was shown to be related to a particular manifestation of the impulsive stimulated Raman scattering mechanism in absorbing materials.[11,12] A significant interest presents the application of the diagnostics with short laser pulses to nanosystems, such as nanoparticles of various shapes.[13–16] In nanomaterials high frequency acoustic modes appear due to confinement of coherent acoustic phonons. Acoustic oscillations reflect the elastic properties, shape, and dimensions of the nanostructure, while optical phonon frequencies depend on the rigidity and the effective mass of the atoms involved in the optical phonon oscillation.

We investigated optical transient responses from samples of Bi nanowires with a femtosecond pump-probe technique. Bi nanowires are of special interest because of their exceptional thermoelectric properties.[17] In nanosystems the surface contribution to the free energy is essential, so that their properties can be size dependent and different from bulk materials.[18] The structure of the electronic density of states and the carrier transport properties of a nanowire, which can be considered as a quasi-one-dimensional quantum system, is also modified compared to the bulk material due to a confinement effect in the lateral directions.[18] The Bi crystalline lattice (A7, $3m$ point group symmetry) presents a distorted simple-cubic structure with two atoms per a primitive cell and is especially sensitive to electronic excitations, shifting the equilibrium lattice position.[19] A short laser pulse excites Raman active modes near the center of the Brillouin zone; for Bi these are the totally symmetric breathing A_{1g} and the doubly degenerate E_g mode.[20] Note that in femtosecond pump-probe experiments with bulk Bi samples the magnitude of the A_{1g} mode was dominant, so that for the observation of the E_g mode an increase in the fluence, a manipulation of the pump/probe polarizations, or lowering the temperature was necessary.[8,21,22] For bulk Te and Bi softening of the lattice and reduction in the optical phonon frequency were observed at high excitation levels.[6,8] We demonstrate detection of both acoustic and optical phonon modes in Bi nanowires excited by femtosecond laser pulses and also consider major factors affecting the dynamics of the optical phonons and changes of their frequency at high excitation levels.

II. EXPERIMENTAL SETUP

For measurements we used femtosecond laser pulses at a central wavelength of 810 nm with a repetition rate of 1 kHz, a pulse energy of up to 0.75 mJ, and a pulse duration of about 50 fs. The initial laser beam was split into two parts. The 90% part was modulated by a mechanical chopper at a frequency of 500 Hz and used as a source of the pump pulses. The 10% beam was directed onto a beta barium borate crystal, and the generated second harmonic at 405 nm was used as a probe. The intensity of each beam was additionally adjusted by optical neutral density filters. The pump and probe beams were focused on the sample into spots with diameters of about 0.6 and 0.4 mm, respectively. The delay between the pump and probe beams was varied by a

[a]Electronic mail: a-kolomenski@physics.tamu.edu.
[b]Also at Microscopy and Imaging Center, Texas A&M University, College Station, Texas 77843-2257.

 © 2008 American Institute of Physics

Downloaded 18 Feb 2010 to 192.195.92.231. Redistribution subject to AIP license or copyright; see http://jap.aip.org/jap/copyright.jsp

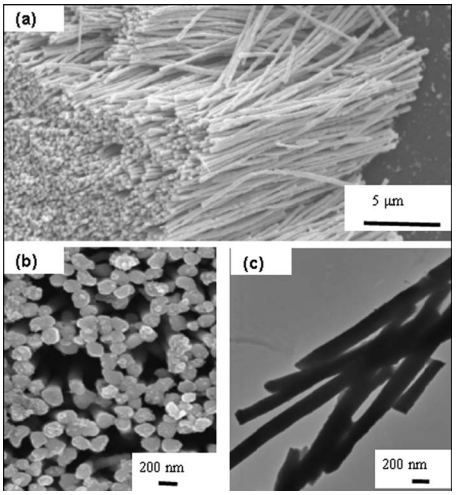

FIG. 1. Investigated Bi nanowires: (a) SEM image of freestanding nanowires, (magnification of 2.6×10^3), (b) SEM image (view of nanowires from top, 1.4×10^4), and (c) TEM image (2×10^4).

computer-controlled translation stage. For transmission measurements at low sample densities a photodiode was used. With high density samples the light scattered from the sample surface in a nonspecular direction was collected by a lens and registered by a cooled photomultiplier. The signal from the photodetector was then measured with a lock-in amplifier.

III. SAMPLES OF NANOWIRES

The samples of Bi nanowires were fabricated by electrochemically depositing metal into the pores of a membrane by a process described in more detail elsewhere.[23] We studied nanowires deposited on a glass substrate (the covered surface fraction of ~10%) and also densely packed freestanding nanowires [see scanning electron microscope (SEM) and transmission electron microscope (TEM) images in Fig. 1]. In the latter case the nanowires were submerged in water to reduce heating. For the nanowires on a substrate, the transmission of the probe beam was measured and for freestanding nanowires the transmission through the sample was below 1%; therefore measurements with the scattered light of the probe beam were performed.

The resultant length of the nanowires was about 15 μm and the filling factor, defined as the volume fraction of the nanowires in the sample, was $f\sim0.5$. From TEM images of Bi nanowires [Fig. 1(c)] the diameters of the nanowires were measured to be $d\approx200\pm20$ nm. The electron diffraction analysis of the crystalline structure shows that nanowires consist of relatively large crystallites with a typical length of about 1 μm.

IV. EXPERIMENTAL RESULTS

The transmission response of a nanowire sample on a glass substrate is shown in Fig. 2. When nanowires were present on the substrate surface, the tail of the response contained terahertz oscillations. The signal from the substrate quickly decreased on a time scale of about 100 fs. After this the signal reflects response of the nanowires, and it was fitted by an expression

$$S(t) = -A\exp\left(-\frac{t}{\tau_1}\right)\cos[2\pi ft(1+\alpha ft)+\varphi] + B\exp\left(-\frac{t}{\tau_2}\right)+C. \quad (1)$$

The fit produced the following values of interest: $\tau_1=0.48$ ps, $f=1.7$ THz, $\alpha=0.13$, $\varphi=0.60$ rad, and $\tau_2=2.1$ ps. The fit is shown in Fig. 2(a) as a solid line and also for the oscillating contribution the first term of Eq. (1) is plotted as a dotted line in the inset.

The optical response of the probe beam *scattered* from a sample of freestranding Bi nanowires is shown in Fig. 3. The energy of the pump pulses at the sample was set to 6 μJ, which corresponded to a relatively low fluence $F=1.5$ mJ/cm^2. The energy of the probe pulses was 100 nJ. The observed signal (curve A) exhibited an initial peak followed by oscillations and was fitted with the same expression of Eq. (1), providing fitting parameters: $\tau_1=283$ ps, $f=7.7$ GHz, $\alpha=0.11$, $\varphi=0.35$ rad, and $\tau_2=278$ ps.

The initial peak was also recorded with a higher temporal resolution, revealing terahertz frequency oscillations in the initial portion of the signal. These high frequency oscillations are shown in the inset of Fig. 3(a) (curve B), and they

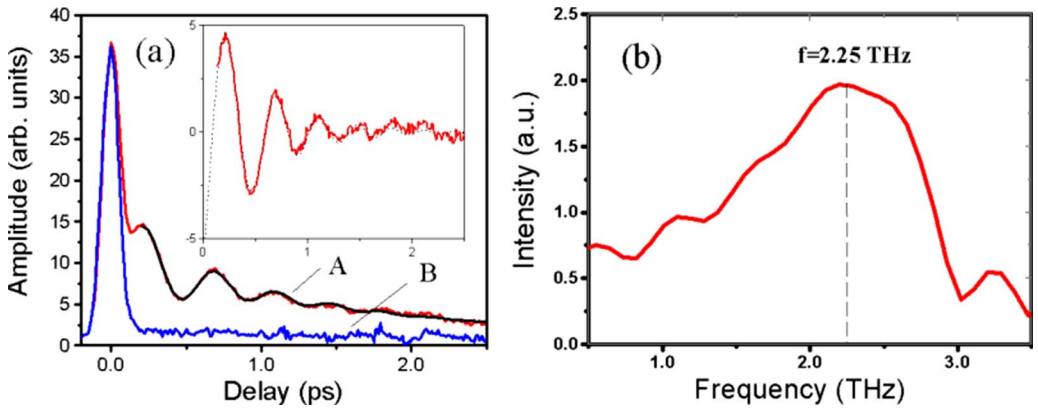

FIG. 2. (Color online) (a) The transmission signal from the Bi nanowires on a glass substrate showing oscillations (curve A) and the signal from a bare substrate (curve B, exhibiting no such oscillations); the laser fluence was $F=10$ mJ/cm^2. The inset shows the oscillating contribution to signal A with a fit shown by a dotted line. (b) The spectrum of the oscillating part of signal A, showing a broad peak around 2.2 THz.

Downloaded 18 Feb 2010 to 192.195.92.231. Redistribution subject to AIP license or copyright; see http://jap.aip.org/jap/copyright.jsp

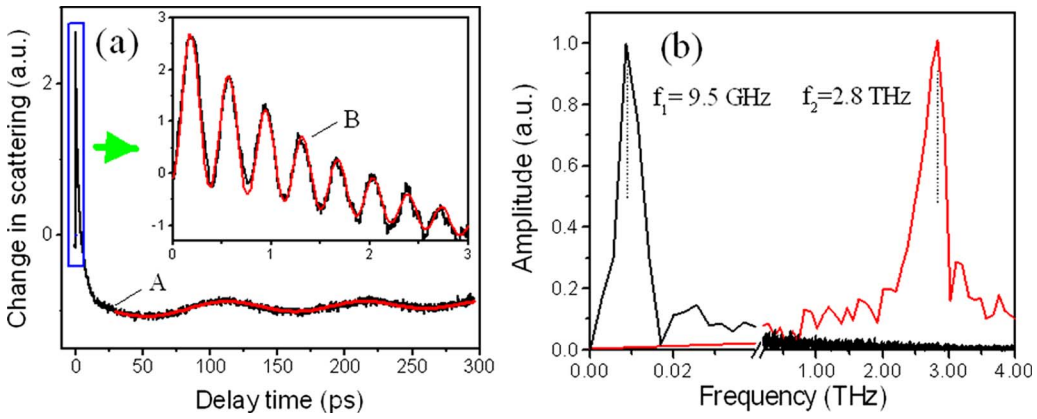

FIG. 3. (Color online) Transient signals of scattered light from Bi nanowires at a relatively low pump fluence of $F=1.5$ mJ/cm^2: (a) the temporal response is shown. For curve A the resolution, determined by the translational speed of the delay line, was set to ~1 ps, and in this case acoustic phonons were detected. For curve B (inset) the resolution was set to ~100 fs; this higher temporal resolution revealed the coherent optical phonon oscillations. (b) Spectral analysis of the oscillating portions of signals A and B: two spectral peaks are observed with maxima at $f_1=9.5$ GHz and $f_2=2.8$ THz.

are characterized by the following fitting parameters: $\tau_1=2.3$ ps, $f=2.6$ THz, $\alpha=0.01$, $\varphi=0.2$ rad, and $\tau_2=2.7$ ps.

The spectrum of the scattered light signals reveals an intensity modulation with two spectral peaks at $f_1=9.5$ GHz and $f_2=2.8$ THz shown in Fig. 3(b). As the following analysis confirms, frequencies $f_{1,2}$ are determined by the excited coherent acoustic and optical phonons, respectively.

V. THEORETICAL DESCRIPTION

To describe the observed signals, we note that coherent acoustic and optical phonon oscillations modulate the dielectric constant of the material,

$$\varepsilon = \varepsilon_0 + \alpha_1 Q_1 + \alpha_2 Q_2, \tag{2}$$

where Q_1 and Q_2 are the lattice displacements corresponding to acoustic and optical phonons and α_1 and α_2 describe the coupling of these oscillations to the material polarization. The acoustic oscillations are related to radial longitudinal eigenmodes of a nanowire. The excitation of optical phonons is produced by the abrupt change in the electronic energy-state distribution function. Both processes can be described by the model of a damped harmonic oscillator,[12,15,24]

$$\frac{\partial^2 Q_{1,2}}{\partial t^2} + \frac{2}{\tau_{d;1,2}}\frac{\partial Q_{1,2}}{\partial t} + \Omega_{1,2}^2 Q_{1,2} = F_{1,2}. \tag{3}$$

In the case of acoustic oscillations Q_1 is the change in the nanowire diameter,

$$F_1 = F_l + F_e;\quad F_l = \Omega_0^2 Q_0 \left[\frac{1}{3B}\gamma C_l (T_l - T_0)\right] g_l(t),$$

$$F_e = \Omega_0^2 Q_0 \left[\frac{2}{9B} C_e(T_e)(T_e - T_0)\right] g_e(t),$$

where $C_{l,e}$ are thermal capacities of the lattice and the electrons, B is the bulk modulus, and the time dependences can be approximated by

$$g_e(t) = \{0, t<0; \exp(-t/\tau_{e\text{-ph}}), t \geq 0\},$$

$$g_l(t) = \{0, t<0; [1-\exp(-t/\tau_{e\text{-ph}})], t \geq 0\},$$

where $\tau_{e\text{-ph}}$ is the thermalization time of the electron-phonon system and γ is the Grüneisen constant of the lattice.[15,24] The two contributions to the force $F_{e,l}$ are due to the impulsive action of the electronic pressure[25,26] and the contribution of the lattice heating. The frequency Ω_1 corresponds to the characteristic radial breathing acoustic mode of the nanowires,

$$f_1 = \Omega_1/2\pi = \xi c_l/\pi d, \tag{4}$$

where the eigen-number $\xi=2.21$ is determined by the boundary problem of radial oscillations of a long rod.[27] Since the impedance of the metal is much larger than the impedance of the surrounding medium $\rho c_{l(\mathrm{Bi})}/\rho c_{l(\mathrm{water})} \approx 25$, the free boundary conditions are valid. Taking the value of the longitudinal sound velocity for a polycrystalline Bi $c_l=2200$ m/s,[28] we obtain from Eq. (4) $f_1=7.75$ GHz, which is within the range of frequencies of the first spectral peak in Fig. 3(b).

It follows from our previous study[23] that the main contribution to the excitation of Bi nanowires comes from the lattice heating. Taking into account only lattice contribution, we obtain for the coherent acoustic vibration after the action of the laser pulse ($t > \tau_0$, where τ_0 is the pulse duration)

$$Q_1 \propto \frac{F_l}{\Omega_1^2}\left[\tilde{g}(0) - \frac{1}{2}\{\tilde{g}(\Omega_{1,+})]e^{-i\Omega_{1,+}t} + \tilde{g}(\Omega_{1,-})e^{-i\Omega_{1,-}t}\}\right], \tag{5}$$

where $\tilde{g}(\omega)$ is the Fourier transform of the normalized temporal dependence of the laser pulse intensity, and $\Omega_{1,\pm} = -i/\tau_{d,1} \pm (\Omega_1^2 - 1/\tau_{d,1}^2)^{1/2}$.

For description of optical phonon oscillations we use Eq. (3) with Q_2 being the displacement of atoms in the optical phonon oscillation. The force F_2 can be found as an average of the electron-phonon coupling operator $F=\langle \Xi \rangle = \Xi_0$.[11,12] This approach takes into account also the resonant interaction of light with the energy levels, causing strong absorption, and expresses the force in terms of a modified Raman tensor.[12] Consequently, the solution of Eq. (2) for $t > \tau_0$ is

Downloaded 18 Feb 2010 to 192.195.92.231. Redistribution subject to AIP license or copyright; see http://jap.aip.org/jap/copyright.jsp

$$Q \propto \frac{\mathrm{Im}(\varepsilon)\Xi_0}{\lambda\Omega_2^2} V N_{\mathrm{ph}} \left\{ \tilde{g}(0) - \frac{1}{2}[\tilde{g}(\Omega_{2,+}) e^{-i\Omega_{2,\pm}t} + \tilde{g}(\Omega_{2,-}) e^{-i\Omega_{2,-}t}] \right\}, \quad (6)$$

where $\mathrm{Im}(\varepsilon)$ is the imaginary part of the dielectric permittivity of the material (Bi), λ is the optical wavelength, V is the irradiated volume, N_{ph} is the flux of incident photons, Ω_2 is the optical phonon frequency, and $\Omega_{2,\pm} = -i/\tau_{d,2} \pm (\Omega_2^2 - 1/\tau_{d,2}^2)^{1/2}$.

For relatively weak damping, $\Omega_{1,2} \gg \tau_{d;1,2}^{-1}$, the amplitude of the oscillation is proportional to the Fourier component of the intensity envelope at the phonon frequency.[9,12] For a short pulse (as in our experiments) $\tilde{g}(\Omega_{1,2}) \approx \tilde{g}(0)$, and the oscillating part of the solution of Eq. (3) for $t \gg \tau_0$ can be presented as a damped cosine function, which corresponds to the oscillating contribution in Eq. (1).

There are several factors that also affect the observed optical response. Electronic excitations produce a contribution to the dielectric function that is changing in time as a result of such processes as thermalization of the electron-phonon system and the recombination of carriers promoted during the excitation to antibonding states. The contribution of these processes is reflected by the second and third terms in the fitting function of Eq. (1).

To clarify the relative roles of different factors on the formation of the optical response related to optical phonons we used the following model. Electronic excitations lead to a softening of the lattice and a redshift of the optical phonon frequency with increasing density of the excitations.[6] The effect of the lattice anharmonicity was considered in Refs. 8 and 29. While in Ref. 8 the optical photon frequency change with the increasing excitation level was mainly attributed to the lattice anharmonicity, the calculations and experiments of Ref. 29 led to conclusion that below $n \approx 1.25\%$, where n is the density of the photoexcited electron-hole plasma expressed as a percentage of the excited valence electrons [for Bi $n=1\%$ corresponds to a carrier density of 1.43×10^{21} cm^{-3} (Ref. 29)], the role of the lattice anharmonicity is small. It was also found that with n approaching $n_c \approx 2.04\%$ the frequency of the optical phonon oscillations, calculated with the model of the displacive mechanism, approaches zero, and the effect of the anharmonicity is essential. At $n \geq n_c$ the energy of the oscillating motion reaches the middle peak (the Peierls distortion[30]) between two valleys in the Bi lattice potential. In the vicinity of this peak, which also somewhat decreases with n, the velocity of the motion decreases, resulting also in the increase of the period of oscillations. The frequency of the small-amplitude oscillations, reflecting the curvature of the potential near the equilibrium position becomes zero at a higher value, $n_{cs} \approx 2.71\%$. To take into account these conclusions we approximated the frequency by the following expression:

$$\Omega(n,A) = \Omega_0 \left\{ 1 - [1 - g_1(n)] \left(\frac{A}{A_{\max}} \right)^2 - [1 - g_2(n)] \left[1 - \left(\frac{A}{A_{\max}} \right)^2 \right] \right\}, \quad (7)$$

where $\Omega_0 = 2\pi f_0$ and f_0 is the optical phonon frequency at the initial temperature [in our experiments this is the room temperature, and we take the frequency value corresponding to the bulk Bi, $f_0 = 2.92$ THz (Refs. 8 and 20)]; A is the amplitude of the optical phonon oscillation and $A_{\max}(n)$ is the maximum value of A for a given n, which is realized just after the excitation, at $t \geq \tau_0$. If $A = A_{\max}$, then $\Omega(n, A_{\max}) = \Omega_0 g_1(n)$ and if $A \geq 0$, then $\Omega(n,A) \geq \Omega_0 g_2(n)$. The functions $g_1(n)$ and $g_2(n)$ were calculated in Ref. 29; however, our calculations have shown that in the region $n \leq 0.5\%$ the decrease in frequency with the functions of Ref. 29 is much smaller compared to experimentally observed one (see further discussion). To account for this, we used the following approximations:

$$g_1(n) = (1 - n/n_c)^{p_1(n)} \quad \text{if } n \leq n_c,$$

$$g_1(n) = 0.5(n/n_c - 1)^{p_1(n)} \quad \text{if } n > n_c,$$

$$g_2(n) = (1 - n/n_{cs})^{p_2(n)} \quad \text{if } n \leq n_{cs},$$

$$g_2(n) = (n/n_{cs} - 1)^{p_2(n)} \quad \text{if } n > n_{cs}, \quad (8)$$

where the power indices $p_1(n) = p_2(n) = \alpha + \beta n$ change linearly with the excitation density. The expressions of Eq. (8) are a generalization of the square root dependence[31] used for description of the red frequency shift of optical phonons in Te. The constants $\alpha = 0.5$ and $\beta = 0.3$ were chosen to provide the average slope of the calculated dependence of Ω on F close to the value following from our observations and those of Ref. 32.

The excitation is strongly inhomogeneous and decays inside the material due to absorption. Since the diameter of the nanowires is much larger than the penetration depth of the optical radiation, we assumed a plane geometry in finding the solution for the diffusion of carriers. Taking into account diffusion and relaxation of the carriers and assuming that the surface recombination is relatively small, the solution for n can be presented in the form

$$n(x,t) = \frac{F}{F_n} \exp\left(\frac{-t}{\tau_r} \right) \int_0^\infty \frac{d\xi \exp(-\xi/l_1)}{(4\pi D t)^{0.5}} \times \left\{ \exp\left[-\frac{(x-\xi)^2}{4Dt} \right] + \exp\left[-\frac{(x+\xi)^2}{4Dt} \right] \right\}, \quad (9)$$

where τ_r is the carrier relaxation time, D is the ambipolar diffusion constant, and l_1 is the penetration depth of the pump beam [$l_1 \approx 22$ nm at 810 nm (Refs. 28 and 33)]. We assumed that n is proportional to the laser energy flux, $n(\%) = F/F_n$, where the value of the normalization constant $F_n = 4.0$ mJ/cm^2, which we estimated from the data of Refs. 29 and 34. We note that estimates based on the results of Ref. 8 gave a close value $F_n = 3.6$ mJ/cm^2. The decay of the optical phonon amplitude is dominated by the relaxation pro-

Downloaded 18 Feb 2010 to 192.195.92.231. Redistribution subject to AIP license or copyright; see http://jap.aip.org/jap/copyright.jsp

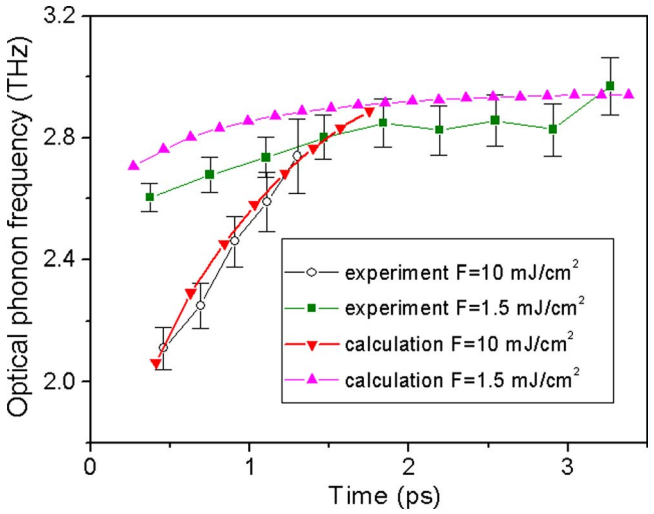

FIG. 4. (Color online) The variations in the optical phonon frequency from experimental data and simulations for $F=10$ and 1.5 mJ/cm^2. The lines connecting experimental points are a guide to the eye.

cess with the time constant τ_d; consequently in Eq. (7) we use $A/A_{\max} \approx \exp(-t/\tau_d)$, and then the signal $S(t)$ is proportional to the integral of the polarization modulation induced by the optical phonon [see Eq. (2)] in the material,

$$S(t) \propto \int_0^\infty dx n(x, t \geq \tau_0) \exp\left(-\frac{t}{\tau_d} - \frac{x}{l_2}\right) \cos[\Omega(x,t)t + \varphi], \tag{10}$$

where $n(x, t \geq \tau_0)$ is the excitation density just after the action of the laser pulse and l_2 is the penetration depth of the probe beam [$l_2 \approx 24$ *nm* at 400 nm (Refs. 33 and 35)]. We assume the response to be proportional to $n(x, t \geq \tau_0)$ since the excitation of the coherent optical phonon occurs as a result of an abrupt change in the density of the excitations, and the following relaxation takes place with characteristic times substantially exceeding the period of the optical phonon. For a purely displacive excitation it holds $\varphi = 0$ [10]; however since the parameters $\Omega\tau_0$ and $1/(\Omega\tau_r)$ are not infinitely small, also a phase shift can appear. With the frequency of optical phonon depending on the excitation level, as in our experiments, the accurate determination of the phase from experimental data becomes difficult, and therefore in calculations the initial phase shift φ was disregarded.

The temporal behavior of the calculated optical phonon frequency is shown in Fig. 4. In the calculations we assumed the carrier relaxation time equal to the decay time of the average component of the signal, determined by the fit to the experimental data [time τ_2 in Eq. (1)]. Thus, we use $\tau_r = 2.1$ ps for $F = 10$ mJ/cm^2 and $\tau_r \approx 2.7$ ps for $F = 1.5$ mJ/cm^2, which are close to the values presented in Refs. 34 and 36. We assume the decay time of the optical phonon equal to the time τ_1, determined by the fit of Eq. (1), thus $\tau_d \approx 0.48$ ps for $F = 10$ mJ/cm^2 and $\tau_d \approx 2.3$ ps for $F = 1.5$ mJ/cm^2. These values are consistent with measurements of Ref. 36. The diffusion coefficient $D = 1.3$ cm^2/s was used for $F = 10$ mJ/cm^2 following the estimate[37] based on the values of mobility measured in Ref. 38 and the Einstein relation as well as the discussion in Refs. 37 and 39. Although the diffusion coefficient tends to decrease with increasing density of excitations, for $F = 1.5$ mJ/cm^2 the photogenerated carriers diffused perpendicular to the length of the nanowires deposited on a substrate, in which case the mobility is expected to be reduced.[40] Therefore we used the same relatively low value $D = 1.3$ cm^2/s also for $F = 1.5$ mJ/cm^2.

VI. DISCUSSION AND CONCLUSIONS

The observation of optical phonons was performed in nanowires deposited on a substrate and with freestanding nanowires. In the first case the transmission signal was measured at a relatively high laser fluence (required in view of the low level of the signal). For freestanding densely packed nanowires the signal of the scattered light was measured, and it contained oscillations from two frequency ranges: around 9.5 GHz and in the interval of 2.1–2.9 THz, which corresponded to acoustic and optical phonons, respectively.

For acoustic phonons the experimentally determined damping coefficient $\gamma = 1/\tau_{d,1}$ includes homogeneous part γ_h due to inherent damping of the material and radiation losses into surrounding medium as well as an inhomogeneous part γ_i. The latter is determined by the size distribution of the nanowires, resulting in dephasing of the oscillations.[24] Estimates show that in our experiments the damping of acoustic phonons was mainly due to the dephasing. Indeed, the estimate of the corresponding time constant $\tau_i \approx (1/\gamma_i) = d/(2\sqrt{2}\pi f \sigma_d)$,[24] where $\sigma_d \approx 20$ nm is the dispersion of the nanowire diameter distribution, gives the decay time $\tau_i \approx 290$ ps, which is close to the experimental value 280 ps.

For optical phonons some inhomogeneous damping can also be expected due to the inhomogeneous excitation of the material; however our simulations have shown that its effect is small for both a relatively small, $F = 1.5$ mJ/cm^2, and high, $F = 10$ mJ/cm^2, laser excitation fluences. We observed a significant reduction in the optical phonon frequency (down to 2.1 THz) and a faster decay at the high excitation levels. The reduction in the frequency was the largest just after the action of the laser pulse. Such redshifts in Bi films down to 2.45 THz (Ref. 8) and even 2.12 THz (Ref. 34) were observed at high excitation levels. The nature of this shift was the subject of discussion[37,39] and a subsequent study.[29] It was suggested[8,39] that the anharmonicity of the lattice potential is mainly responsible for the observed shifts. According to Refs. 29 and 37 the effect of the anharmonicity in Bi is much smaller and practically negligible for $n \leq 1.25\%$; however for higher excitation levels [as in our case for $F = 10$ mJ/cm^2 ($n = 2.5\%$)] the influence of the anharmonicity can be noticeable.

We developed a model taking into account the softening of the lattice and its anharmonicity, inhomogeneity of the excitation, and relaxation and diffusion of carriers. This model reasonably well described the observed dynamics of the optical phonon frequency. As it follows from the results of Ref. 29, the anharmonicity effect plays a minor role at almost all excitation densities of interest, except for a relatively narrow interval in the vicinity of the critical density of excitations n_c, at which the frequency becomes zero. There-

Downloaded 18 Feb 2010 to 192.195.92.231. Redistribution subject to AIP license or copyright; see http://jap.aip.org/jap/copyright.jsp

fore except for this interval of the excitation densities close to n_c (this value also somewhat changes due to anharmonicity) the inhomogeneity of the excitation and the carrier relaxation and diffusion mostly account for the observed dynamics of photoexcited optical phonons. We used approximation for the dependence of the optical phonon frequency on the density of the excitations somewhat different from the one calculated in Ref. 29 to better account for the slope of the dependence $\Omega(n)$ for relatively small n. For $n \approx 0.22\%$ ($F \approx 0.9$ mJ/cm^2) the measured average slope $\Delta\Omega/\Delta F \approx -0.17$ THz/(mJ/cm^2) (Ref. 32) is close to the calculation with our model, $\Delta\Omega/\Delta F \approx -0.14$ THz/(mJ/cm^2), while $\Omega(n)$ of Ref. 29 (which account for inhomogeneous excitation and diffusion) gives a significantly lower value, $\Delta\Omega/\Delta F \approx -0.014$ THz/(mJ/cm^2). Note that the inhomogeneity of the excitation effectively reduces the observed frequency shift because the signal is observed from the penetration depth of the laser radiation including layers with a smaller excitation density.

In conclusion, with the femtosecond two-color pump-probe technique the simultaneous excitation of acoustic and optical phonons in Bi nanowires was registered. The presence of nanowires on a glass substrate resulted in a modulation of the transmitted probe beam at the optical phonon frequency. The transient responses were also measured for freestanding Bi nanowires, in which case both coherent acoustic and optical phonons were detected. The frequencies of the latter decreased with increasing laser fluence. The frequency of the acoustic breathing mode was close to the value calculated from the equation for eigenvalues of the oscillations with a longitudinal velocity corresponding to polycrystalline Bi. The developed model of the optical phonon dynamics accounted for softening and anharmonicity of the lattice, inhomogeneity of the excitation, as well as for relaxation and diffusion of the carriers. It reasonably well described the observed optical phonon frequency downshift for relatively low as well as for high excitation levels. Note that the parallel observation of the acoustic and optical phonons can be also useful in establishing quantitative relations between the main parameters responsible for these processes.

ACKNOWLEDGMENTS

This work was supported by the Robert A. Welch Foundation under Grant Nos. A1546 and A1562 and by NSF under Grant Nos. DMR-0551813, DMR-0606529 and MRI-0722800 and by the Qatar National Research Fund, Grant NPRP30-6-7-35. The FE-SEM acquisition was supported by the NSF under Grant No. DBI-0116835.

[1] W. Hayes and R. London, *Scattering of Light by Crystals* (Wiley, New York, 1978).
[2] J. S. Lannin, J. M. Calleja, and M. Cardona, Phys. Rev. B **12**, 585 (1975).
[3] C. Thomsen, J. Strait, Z. Vardeny, H. J. Maris, J. Tauc, and J. J. Hauser, Phys. Rev. Lett. **53**, 989 (1984); C. Thomsen, H. T. Grahn, H. J. Maris, and J. Tauc, Phys. Rev. B **34**, 4129 (1986).
[4] A. M. Weiner, D. E. Leaird, G. P. Wiederrrecht, and K. A. Nelson, J. Opt. Soc. Am. B **8**, 1264 (1991).
[5] W. A. Kutt, W. Albrecht, and H. Kurz, IEEE J. Quantum Electron. **28**, 2434 (1992).
[6] S. Hunsche, K. Wienecke, T. Dekorsy, and H. Kurz, Phys. Rev. Lett. **75**, 1815 (1995).
[7] M. Hase, K. Mizoguchi, H. Harima, and S.-I. Nakashima, Phys. Rev. B **58**, 5448 (1998).
[8] M. Hase, M. Kitajima, S. Nakashima, and K. Mizoguchi, Phys. Rev. Lett. **88**, 067401 (2002).
[9] Y.-X. Yan and K. A. Nelson, J. Chem. Phys. **87**, 6240 (1987).
[10] H. J. Zeiger, J. Vidal, T. K. Cheng, E. P. Ippen, G. Dresselhaus, and M. S. Dresselhaus, Phys. Rev. B **45**, 768 (1992).
[11] G. A. Garrett, T. F. Albrecht, J. F. Whitaker, and R. Merlin, Phys. Rev. Lett. **77**, 3661 (1996).
[12] T. E. Stevens, J. Kuhl, and R. Merlin, Phys. Rev. B **65**, 144304 (2002).
[13] M. Nisoli, S. De Silvestri, A. Cavalleri, A. M. Malvezzi, A. Stella, G. Lanzani, P. Cheyssac, and R. Kofman, Phys. Rev. B **55**, R13424 (1997).
[14] J. Hodak, A. Henglein, and G. Hartland, J. Chem. Phys. **111**, 8613 (1999).
[15] C. Voisin, N. Del Fatti, D. Christofilos, and F. Vallee, Appl. Surf. Sci. **164**, 131 (2000).
[16] M. Hu and G. V. Hartland, in *Nanoscale Materials*, edited by L. M. Liz-Marzan and P. V. Kamat (Kluwer, Norwell, 2003), pp. 97–118.
[17] M. S. Dresselhaus, Y. M. Lin, O. Rabin, A. Jorio, A. G. Souza Filho, M. A. Pimenta, R. Saito, G. Samsonidze, and G. Dresselhaus, Mater. Sci. Eng., C **23**, 129 (2003).
[18] Y. M. Lin, X. Sun, and M. S. Dresselhaus, Phys. Rev. B **62**, 4610 (2000).
[19] D. B. Smith, "Lattice dynamics of bismuth," Ph.D. thesis, University of New Mexico, 1968).
[20] P. H. Dederichs, H. Schober, and D. J. Sellmyer, *Phonon States of Elements, Electron States and Fermi Surfaces of Alloys*, edited by K.-H. Helwege and J. L. Olsen, Landolt-Börnstein, New Series, Group III, Vol. 13, Pt. A (Springer, New York, 1981).
[21] M. Hase, K. Mizoguchi, H. Harima, S. Nakashima, M. Tani, K. Sakai, and M. Hangyo, Appl. Phys. Lett. **69**, 2474 (1996).
[22] K. Ishioka, M. Kitajima, and O. V. Misochko, J. Appl. Phys. **100**, 093501 (2006).
[23] S. N. Jerebtsov, Al. A. Kolomenskii, H. Liu, H. Zhang, Z. Ye, Z. Luo, W. Wu, G. G. Paulus, and H. A. Schuessler, Phys. Rev. B **76**, 184301 (2007).
[24] G. V. Hartland, J. Chem. Phys. **116**, 8048 (2002).
[25] V. E. Gusev, Opt. Commun. **94**, 76 (1992).
[26] M. Perner, S. Gresillon, J. März, G. von Plessen, J. Feldmann, J. Porstendorfer, K.-J. Berg, and G. Berg, Phys. Rev. Lett. **85**, 792 (2000).
[27] M. Hu, X. Wang, G. V. Hartland, P. Mulvaney, J. P. Juste, and J. E. Sader, J. Am. Chem. Soc. **125**, 14925 (2003).
[28] Y. Eckstein, A. Lawson, and D. Reneker, J. Appl. Phys. **31**, 1534 (1960).
[29] É. D. Murray, D. M. Fritz, J. K. Wahlstrand, S. Fahy, and D. A. Reis, Phys. Rev. B **72**, 060301(R) (2005).
[30] R. Peierls, *More Surprises in Theoretical Physics* (Princeton University Press, Princeton, 1991).
[31] S. Hunsche and H. Kurz, Appl. Phys. A: Mater. Sci. Process. **65**, 221 (1997).
[32] A. Q. Wu and X. Xu, Appl. Surf. Sci. **253**, 6301 (2007).
[33] J. C. G. de Sande, T. Missana, and C. N. Afonso, J. Appl. Phys. **80**, 7023 (1996).
[34] K. Sokolowski-Tinten, C. Blome, J. Blums, A. Cavalleri, C. Dietrich, A. Tarasevitch, I. Uschmann, E. Förster, M. Kammler, M. Horn-von-Hoegen, and D. von der Linde, Nature (London) **422**, 287 (2003); M. Hase, K. Ishioka, M. Kitajima, S. Hishita, and K. Ushida, Appl. Surf. Sci. **197–198**, 710 (2002).
[35] *Semiconductors: Crystal and Solid State Physics*, Landolt-Börnstein, New Series, Group III, Vol. 17, Pt. A, edited by O. Madelung (Springer, Berlin, 1983).
[36] M. F. DeCamp, D. A. Reis, P. H. Bucksbaum, and R. Merlin, Phys. Rev. B **64**, 092301 (2001).
[37] S. Fahy and D. A. Reis, Phys. Rev. Lett. **93**, 109701 (2004).
[38] E. I. Rogacheva, S. N. Grigorov, O. N. Nashchekina, S. Lyubchenko, and M. S. Dresselhaus, Appl. Phys. Lett. **82**, 2628 (2003).
[39] M. Hase, M. Kitajima, S. Nakashima, and K. Mizoguchi, Phys. Rev. Lett. **93**, 109702 (2004).
[40] L. Li, Y. W. Yang, X. H. Huang, G. H. Li, R. Ang, and L. D. Zhang, Appl. Phys. Lett. **88**, 103119 (2006).

Downloaded 18 Feb 2010 to 192.195.92.231. Redistribution subject to AIP license or copyright; see http://jap.aip.org/jap/copyright.jsp